Characterization of Nonthermal Focused Ultrasound for Noninvasive Selective Fat Cell Disruption (Lysis): Technical and Preclinical Assessment

Spencer A. Brown, Ph.D.
Lior Greenbaum, Ph.D.
Stella Shtukmaster, M.S.
Yehuda Zadok
Shmuel Ben-Ezra
Leonid Kushkuley, Ph.D.

Dallas, Texas; and Yoqneam, Israel

Background: There has been a lack of published bench and preclinical data supporting the safety and effectiveness of a noninvasive, nonthermal, focused ultrasound technology for body contouring.
Methods: A series of experiments were conducted with a transcutaneous focused ultrasound device (UltraShape Contour I; UltraShape Inc., Yoqneam, Israel): (1) three-dimensional acoustic field distribution was measured by hydrophone in a water bath; (2) the real-time two-dimensional acoustic field was assessed using optical visualization by a Schlieren system; (3) three-dimensional and Schlieren results were compared in tissue-mimicking gel phantoms and in frozen specimens of porcine subcutaneous fat; and (4) a porcine in vivo preclinical model was used to test safety, selectivity, and efficacy by histological staining of excised skin and subcutaneous fat specimens.
Results: Real-time imaging of acoustic field distribution obtained by the Schlieren system, as well as real-time ultrasound visualization, produced stable cavitation both in water and in the gel phantoms. The area where the effect was visible corresponded to the focal area of energy delivered by the system transducer, as measured by the hydrophone. Histologically stained specimens of skin and subcutaneous fat that were excised from porcine studies ($n = 14$) following treatments ($n = 31$) demonstrated fat cell lysis and no observable cellular destruction of adjacent blood vessels, nerves, and connective tissue. No epidermal or dermal changes were observed clinically or histologically.
Conclusions: The delivery of noninvasive focused ultrasonic energy has been validated and supported by the basic and preclinical data presented. Future studies will investigate various treatment regimens for improved body-contouring results. (*Plast. Reconstr. Surg.* 124: 92, 2009.)

A growing number of people in the United States seek cosmetic solutions for the removal of excess weight. Surgically, the number of patients receiving abdominoplasties has increased from 62,713 to 148,410 in 2007.[1] The same trend was observed with brachioplasty procedures, with a 4041 percent increase during the same time period. With the desire to improve body contours, additional surgical procedures such as liposuction have allowed the removal of excess fat tissues in specific body areas for shaping the body. This procedure, along with modifications (ultrasound-assisted and laser-assisted liposuction), has provided satisfactory results for many people. But liposuction is a surgical procedure and as such has limitations and possible complications. A range of death rates attributable to liposuction have been reported, and one report states that the death rate from liposuction is similar to that for car accidents (16 per 100,000).[2,3] Complications can include

From the Department of Plastic Surgery, University of Texas Southwestern Medical Center, and UltraShape Inc.
Received for publication September 21, 2008; accepted January 13, 2009.

DOI: 10.1097/PRS.0b013e31819c59c7

Disclosures: *Spencer A. Brown, Ph.D., is a member of the North America Medical Advisory Board of UltraShape Inc., Yoqneam, Israel. Lior Greenbaum, Ph.D., Stella Shtukmaster, M.S., Yehuda Zadok, Shmuel Ben-Ezra, and Leonid Kushkuley, Ph.D., are employees of UltraShape Inc.*

infections, embolism, visceral perforations, seroma, nerve compression, changes in sensation, swelling, skin necrosis, burns (in ultrasound- or laser-assisted liposuction), fluid imbalance, toxicity from anesthesia, scars, and contour irregularities. Cost is also an issue.

Currently, noninvasive alternatives to liposuction involve lifestyle changes in diet and exercise and/or acceptance of one's body as it is. Mesotherapy or multiple injections of bile salt solutions have been used but are currently not approved by the U.S. Food and Drug Administration.[4] Although commercially available creams, lasers, and so on have advertised fat loss upon application, only one Food and Drug Administration–approved technology that uses bipolar radio frequency and optical energy (either laser or light) has been approved to treat the appearance of cellulite but not underlying fat.[5]

Novel applications using ultrasound without surgical intervention have been investigated to deliver an energy signature through the skin. Noninvasive ultrasonic energy may be delivered to the tissue in one of two forms: nonfocused or focused waves. For nonfocused ultrasonic energy delivery, skin and subcutaneous fat are exposed to approximately the same extent (Fig. 1, *above*). Due to ultrasound attenuation, signal energy decreases with distance; as a result, the skin is exposed to maximum energy intensity. In contrast, focused ultrasound can be concentrated in a defined subcutaneous focal area to produce fat cell lysis and limit damage to blood vessels, nerves, connective tissue, and muscles (Fig. 1, *below*).

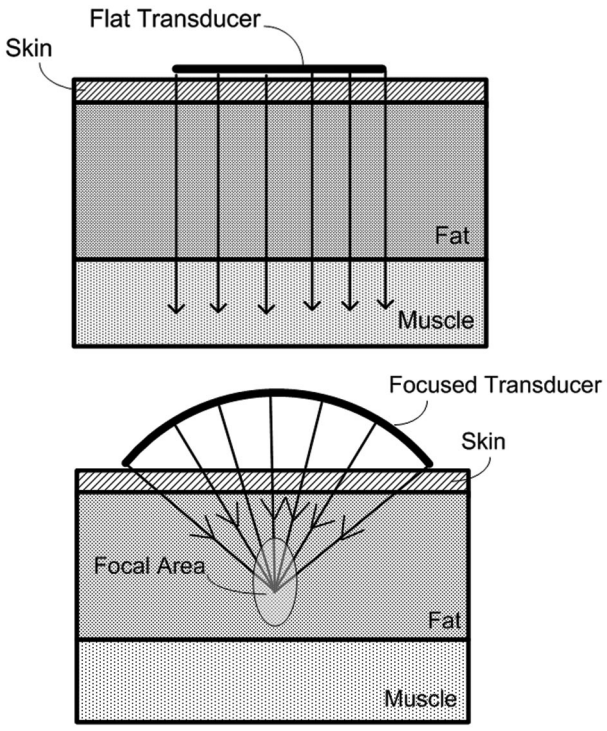

Fig. 1. Illustrations of the ultrasound beam extension when energy is emitted from a flat (*above*) or focused (*below*) transducer.

We report here the basic science results and validation of a transcutaneous focused ultrasound device, using acoustic field measurements, visualization, and preclinical characterization of specific tissue effects produced by the system. Results of previous clinical studies have been published elsewhere.[6,7]

MATERIALS AND METHODS

Device

The transcutaneous focused ultrasound device (Contour I; UltraShape, Inc., Yoqneam, Israel) is composed of a transducer, a power control unit, and a tracking and guidance system. The transducer itself includes a therapeutic focused transducer for ultrasound energy delivery, an echo-mode transducer for monitoring acoustic contact, and temperature sensors for temperature control. The therapeutic focused transducer applies focused ultrasound energy to a target area and is connected to the power unit, which consists of an electronic means for energizing the therapeutic focused transducer and echo-mode transducer, executing modes of operation, and so on. The three-dimensional tracking and guidance system directs an operator to move the transducer over the target treatment area to ensure smooth, uniform body-contouring results (Fig. 2).

Acoustic Field Distribution

The geometric and temporal distributions of ultrasonic sound intensity waves can be characterized as focused or unfocused acoustic field parameters (pressure, power, intensity, and so on) measured by a calibrated hydrophone in a water bath tank.[8] As an ultrasound transducer radiates energy into the water, the hydrophone is moved from point to point within specified planes. At each point, acoustic pressure is measured and recorded and two- and three-dimensional field distributions are calculated. The measurements are made in two planes parallel to the face of the transducer at distances of 1 mm and 14 mm. The plane at 14 mm is a focal plane, in which acoustic pressure achieves maximum value. During the measuring phase, the transducer is run by 4.0 W of electric power.

Schlieren Real-Time Imaging

Visual observations of ultrasonic energy (focused or unfocused) as Schlieren patterns is a well-estab-

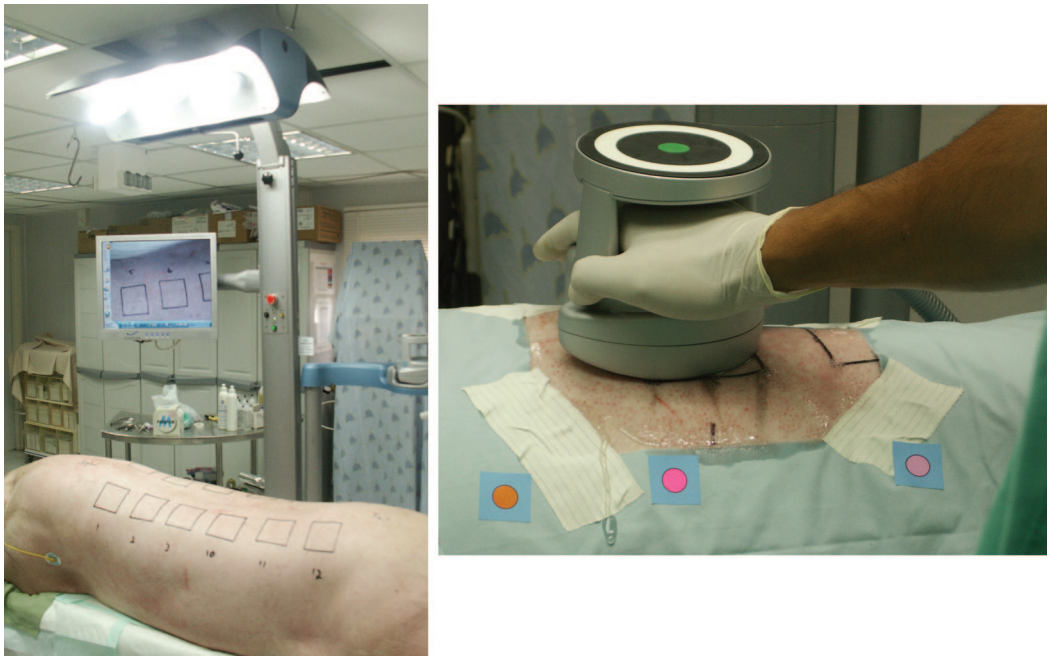

Fig. 2. Porcine ultrasonic treatment. (*Left*) Areas to be treated are marked and defined in the system before treatment is carried out. (*Right*) The ultrasound transducer is placed on the area to be treated, and each treatment uses the commercial setting and treatment protocols suggested by the vendor.

lished technique. Two-dimensional real-time acoustic field distributions are based on the phenomenon of light diffraction by ultrasound waves in a transparent medium.[9] An ultrasound beam produces a variable density grating (inhomogeneity) in the medium, with spacing equal to the sound wavelength. When a beam of light is propagating in the medium, perpendicular to the acoustic beam, it is refracted by the medium density inhomogeneities and produces an image of acoustic field distribution in real time on the screen (or sensor of a digital camera). The intensity of the image is proportional to the acoustic power of the beam.[10]

Phantom

As a human skin model equivalent, a gelatin (10%, m/v; Sigma-Aldrich, St. Louis, Mo.) was prepared in water, heated to 60°C for 15 minutes, transferred into a plastic container, and stored at 4°C until ready for use. To visualize the effect in the phantom, an ultrasound imager (Diasus; Dynamic Imaging, Livingston, Scotland, U.K.) with an 8-MHz imaging ultrasound transducer is operated simultaneously to record acoustic field distributions in real time.

Animal Experimental Approach

The domestic adult male pig, *Sus scrofa domestica* (Landrace, 325 to 375 lbs), was used in this study (Fig. 2).

Histology

Freshly isolated porcine skin specimens were immediately frozen in liquid nitrogen and sectioned in a cryostat for examinations of acute tissue changes after treatment. For more defined histological analysis of tissues for staining procedures, tissue samples were excised immediately and transferred in 4% (m/v) paraformaldehyde solution. After 60 minutes, specimens were transferred to a second incubation in the same solution for 3 days. Sections on slides were stained using protocols for either hematoxylin and eosin or Masson's trichrome.[11,12]

Lactate Dehydrogenase Activity

Acutely excised tissue specimens were transferred into an incubation solution of 1 ml of reduced α-nicotinamide adenine dinucleotide (2.5 mg/ml in H_2O), 2.5 ml of ρ-nitro-blue tetrazolium chloride (2 mg/ml in H_2O), 1 ml of phosphate-buffered saline (pH 7.4) (2 mg/ml in diluted H_2O), and 0.5 ml of lactate-free Ringer's solution from stock (25% dilution, v/v) for 15 minutes or until brown color developed and digital images were recorded.[13] All materials were obtained from Sigma-Aldrich.

RESULTS

Acoustic field distribution measurements in water produced concentric rings of very low power distributions of focused ultrasonic energy signatures

on the transducer-fluid interface, with a maximum pressure of 120 kPa (Fig. 3, *above, left*). The ratio of the acoustic pressure in the focus to maximal pressure on the skin was in the range 3.5 to 4.0 (Fig. 3). The dimensions of the focal length and the focal diameter (as calculated at 50 percent of the maximum peak pressure level) were 24 mm and 6 mm, respectively. In contrast, at the greater depth of 14 mm, a tightly focused ultrasonic energy beam was delivered in a focal region with a maximum pressure value (450 kPa) (Fig. 3, *below, left*).

In addition to these measurements, real-time optical visualization of the acoustic field was performed using a Schlieren system in the fluid medium in the plane perpendicular to the transducer face (Fig. 4, *above*). Two cones emanating from the transducer-fluid interface (Fig. 4, *above*) corresponded to visible concentric rings (Fig. 3, *above, left*). The bright oval area corresponded to the focal region as shown in Figure 3. The brightest part of the focal region corresponded to the focus of the acoustic field and was approximately 15 mm from the transducer-fluid interface. Focal region dimensions were 20 mm for the focal length and 8 mm for the focal diameter. The recorded values were in good agreement with recorded measurements from the hydrophone protocol. Using an ultrahigh speed camera, digital images of air bubbles were captured after one ultrasonic pulse. The air bubbles were concentrated only in the focal region, where the pressure was higher than in surrounding areas (Fig. 4, *above*). No air bubble formation was observed in any other region of the fluid.

A gel phantom model was used to assess the effect of ultrasound on a testing medium that was more consistent with skin and fat densities, unlike the fluid environments tested previously. Assessments were performed using ultrasound visualization in a gelatin medium. The ultrasound transducer transmitted energy perpendicularly to an ultrasound imaging transducer. The treatment focal length was 18 mm, with a focal diameter of 9 mm. An area of bright spots corresponded to the air bubbles produced in the gel model, and no perturbations of the gel were observed at the transducer-gel interface or at gel depths below the area of bubble formation (Fig. 4, *below*).

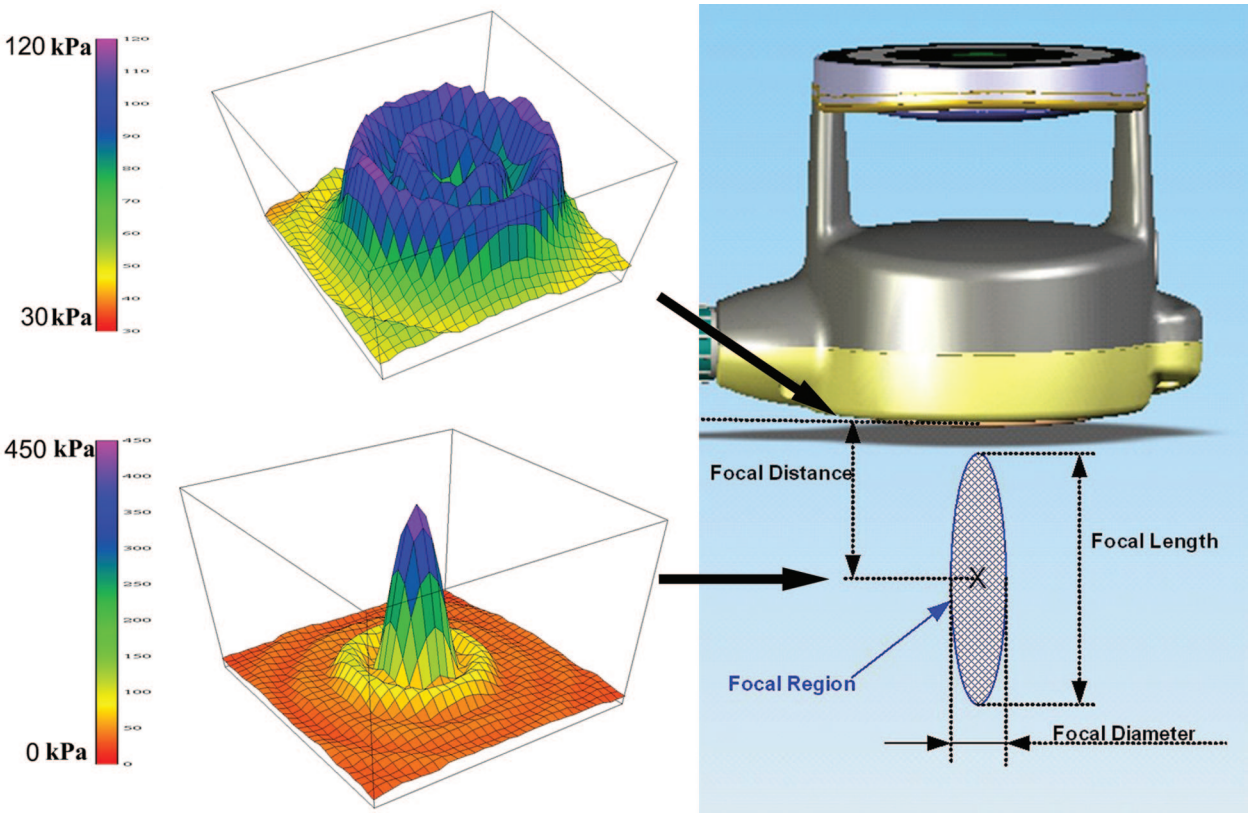

Fig. 3. Acoustic field distribution of the focused ultrasound energy. The focal distance was defined as the distance between the transducer surface and the focal point (14 mm), whereas the focal point is the point in which the pressure level is maximum (the "*X*" in the center of the focal length).

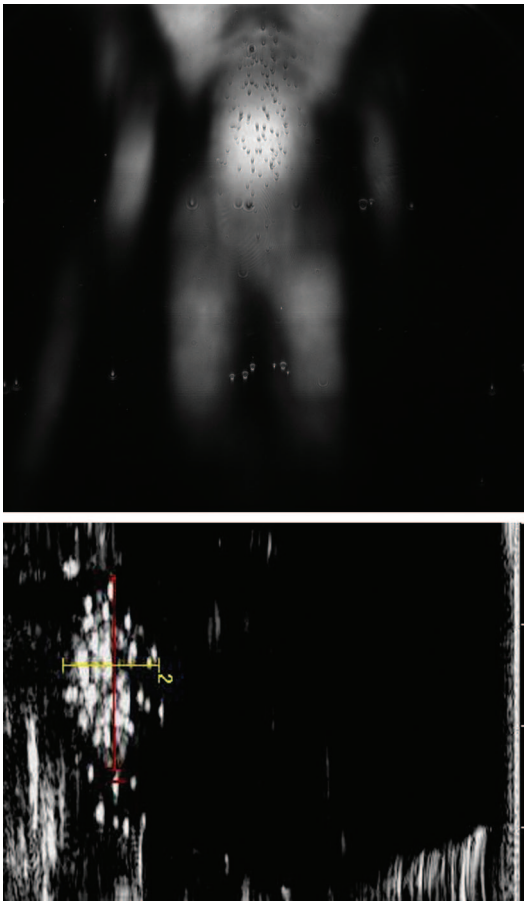

Fig. 4. Visualization of the focused ultrasound. The Schlieren system was used to visualize the effect of a single ultrasound pulse (*above*). A bubble cloud was seen in the focal area, where maximum acoustic pressure is obtained (*red window*). A similar result was obtained when the ultrasound energy was transmitted into a tissue-mimicking phantom, as detected by an imaging ultrasound system (*below*).

In animal experiments, porcine skin was treated and removed immediately to characterize the acute tissue effects of the delivered ultrasonic energy. Clinically, no effect on skin color or adverse events were observed using either single pulses or entire skin areas comprising a treatment zone (data not shown). Histologically, no differences were distinguishable using complete treatment procedures on the skin from untreated or ultrasonically treated specimens in keratinocytes or fibroblasts, as observed in Figure 5, or in hair follicles, sweat glands, and the organization of the extracellular matrix (data not shown).

Staining the excised ultrasonically treated skin specimens immediately with lactate dehydrogenase demonstrated that epidermal and dermal levels were stained, denoting cell viability (Fig. 6). In contrast, specimens from the ultrasonically treated porcine skin had unstained subcutaneous fat layers that were approximately 10 mm in depth.

To further characterize the nature of the injury to the subcutaneous layer of ultrasonically treated skin, acutely isolated tissue specimens were frozen immediately and sectioned (Fig. 7). The untreated specimens had normal and undisturbed subcutaneous adipocytes after a single ultrasonic pulse (Fig. 7). In treated skin specimens, a defined area of tissue destruction, with a focal length of 10 mm and a focal diameter of 6 mm, was observed as a cluster of small holes (approximately 1 mm in diameter). From histological staining, cell-type selectivity was examined and showed that adipocyte lysis was observed and that loss of membranes of adjacent cells created holes in each of the treated porcine skin specimens (Fig. 8, *center* and *below*). Connective tissue, blood vessels, and nerves had no observable damage by hematoxylin and eosin and Masson's trichrome staining techniques, and no coagulation of cells or extracellular matrix components were noted. In the untreated skin specimens (Fig. 8, *above*), all tissue components remained intact.

DISCUSSION

The data shown here from a sophisticated series of physics modeling systems, a preclinical model, and subsequent histological analysis demonstrated the specific delivery of a noninvasive energy signature that generated a defined high-energy treatment zone. Furthermore, the ultrasonic energy was delivered and reacted with the modeling medium in the formation of bubbles or cavitation. Translated to the porcine preclinical animal model in 14 animals, the treatment area using multiple pulses showed that single pulses of ultrasonic energy generated cavitation-like areas with well-defined treatment zones. As with the laboratory modeling systems, there was no evidence of ultrasonic energy delivered at the transducer-skin interface, which would have the potential to produce adverse events in the dermis. In the treatment zones, adipocytes were destroyed with little or no observable damage to associated nerves and blood vessels. There is no histological support for thermal destruction of dermal tissue or adipocytes with the focused ultrasound treatments.

Ultrasound is widely used in medicine for diagnostic and therapeutic applications.[14–16] Contrary to ultrasound imaging, therapeutic ultrasound is not so widely used, though it can induce a vast range of biological effects at very different acoustic parameters. At low levels, beneficial, reversible cellular effects can be produced, whereas at higher intensities, instantaneous cell death can occur. Accordingly,[16]

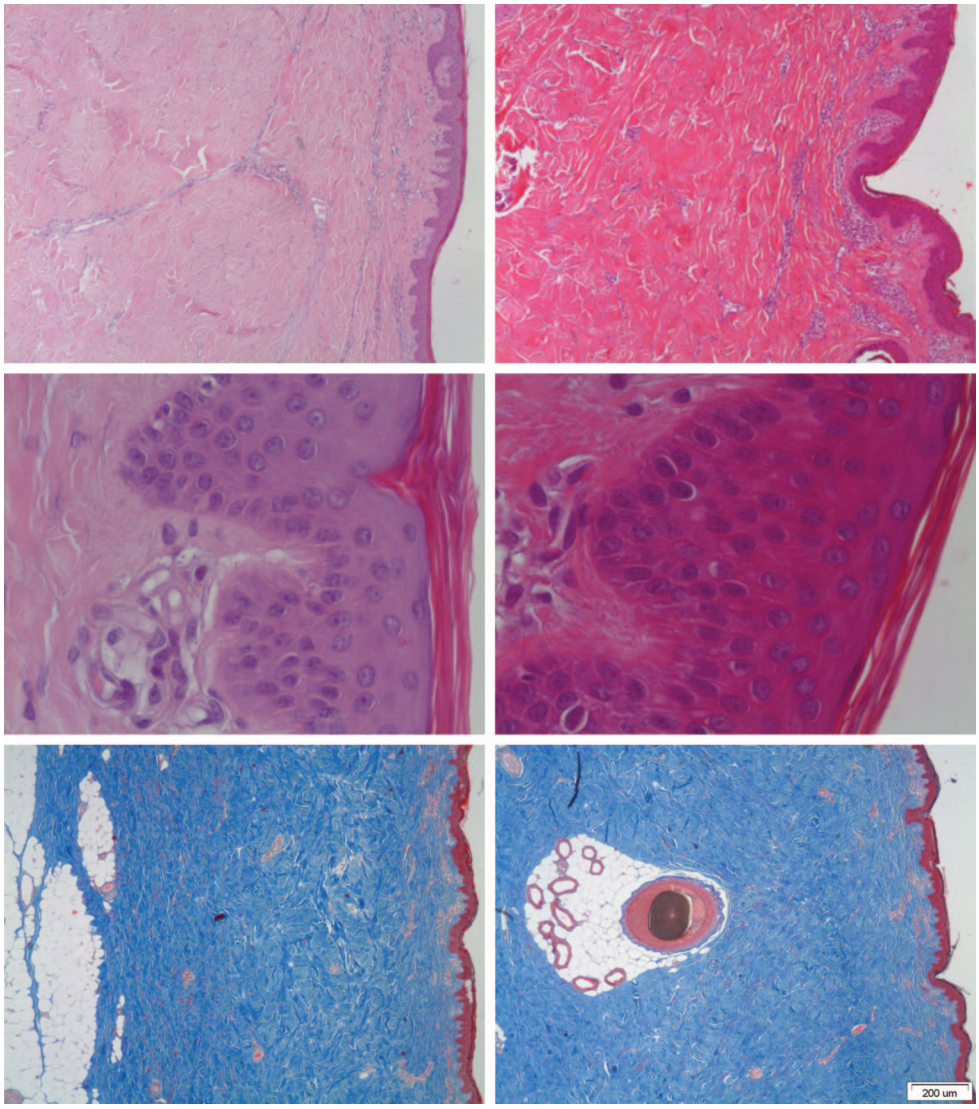

Fig. 5. Safety evaluation demonstrated on skin tissue. The histology was processed using the paraffin-embedding technique. (*Above, left and right,* and *center, left*) Untreated tissue; (*center, right,* and *below, left and right*) treated tissue. (*Above, left and right*; *center, right*; and *below, left*) Hematoxylin and eosin stain; (*center, left*, and *below, right*) Masson's trichrome stain.

ultrasound therapies can be broadly divided into two groups: "high"-power and "low-"power therapies. At the one end of the spectrum, high-power applications include high-intensity focused ultrasound and lithotripsy, whereas at the other end, low-power applications include sonophoresis, sonoporation, gene therapy, and bone healing. Most therapeutic applications use heating to achieve the required effect. In the case of low-power ultrasound, raising the temperatures above normothermic levels by a few degrees may have a number of beneficial effects, such as increasing the blood supply to the affected area. In high-power ultrasound, tissue temperatures are raised very rapidly (typically in less than 3 seconds) to in excess of 56°C, causing instantaneous cell death.

The initial steps to understand and characterize the transcutaneous focused ultrasound device were performed on the laboratory bench using state-of-the-art physics methodologies. Employing acoustic field distribution measurements in a fluid system, single ultrasonic pulses demonstrated very low power levels at the transducer-fluid interface. The energy was distributed uniformly and broadly over the entire surface and not characterized by spikes or peaks. The same results were observed using either the Schlieren optical system in a fluid medium or the tissue-mimicking gel phantom model. At greater depths, significant levels of defined focal ultrasonic energy concentrations were identified using all three laboratory bench proto-

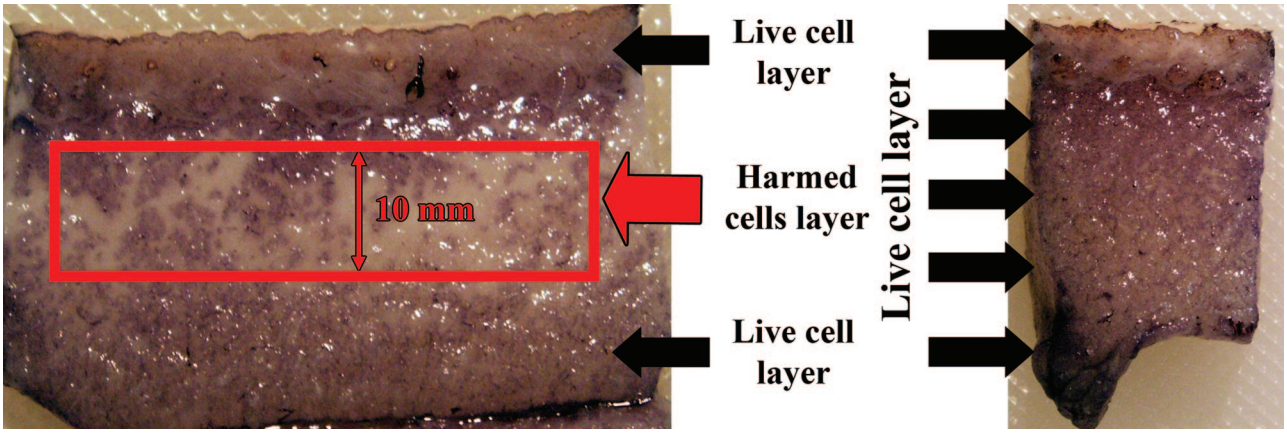

Fig. 6. Gross evaluation of transcutaneous focused ultrasound on the swine adipose tissue. The photographs represent treated tissue (*left*) and untreated tissue (*right*). Lactate dehydrogenase activity staining was performed on both treated and untreated tissues, whereas the indication for cellular damage is seen only in the treated tissue, in the subcutaneous fat layer.

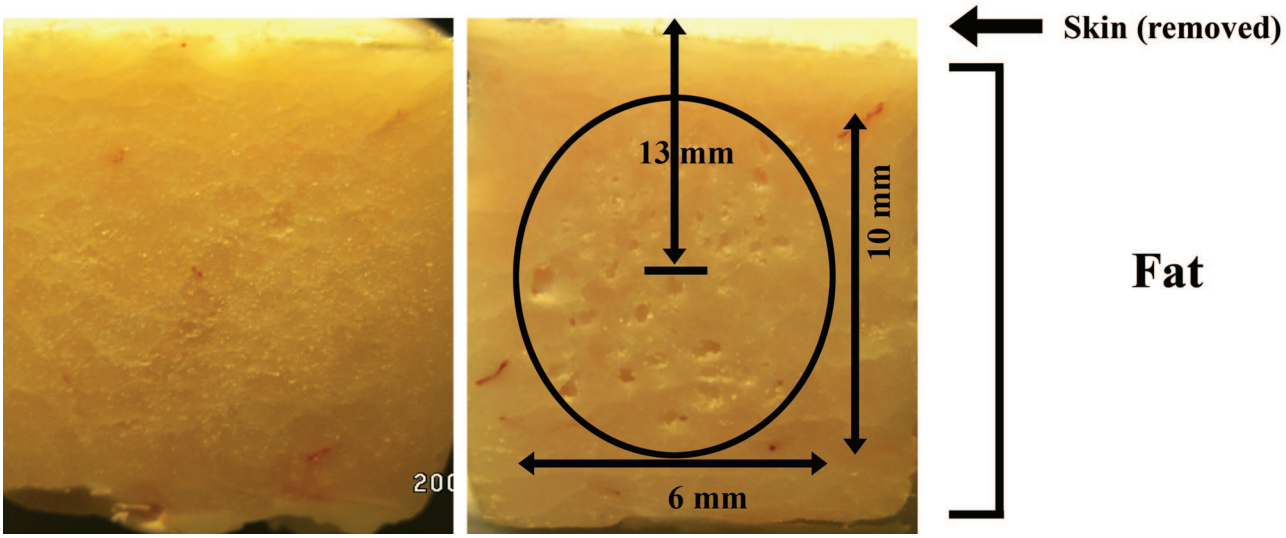

Fig. 7. Destructive zones following ultrasonic treatment in a porcine model. At the end of an entire treatment (more than 300 pulses), the adipose tissue was excised and immediately frozen in liquid nitrogen. The ultrasound effect in the tissue resulted in small (<1.0 mm) holes (*right*) that were not present in untreated tissue (*left*).

cols. Below the optically defined ultrasonic focal zones of energy, no concentrated ultrasonic acoustic energy patterns were observed. In summary, a focused ultrasonic energy pattern of definable boundaries below the depth of the transducer-model surface interface was characterized. Very low acoustic energy levels were associated with the transducer-model interface and were below the defined target treatment zone.

Of considerable interest is the characterization of the form of energy that would be imparted to the treated materials or tissue. From a physics viewpoint, energy can be delivered as thermal energy, mechanical energy, or cavitation. The term cavitation refers to a range of complex phenomena that involve the creation, oscillation, growth, and collapse of bubbles within a medium[14–17] to subsequently produce mechanical energy. In this application, tissue destruction is considered to be uniquely derived from mechanical energy. This is further substantiated by the digital images of a bubble cloud formation at treatment dimensions similar to those obtained from single ultrasonic pulses in both the Schlieren and gel phantom laboratory model systems. More importantly, a well-defined cluster of destructive "bubbles" or small areas of approximately 1 mm were observed after treating skin with one ultrasonic pulse. Further histological analysis showed that the boundaries of the ultrasonic injury zones of adipocytes were consistent with mechanical injury and not thermally in-

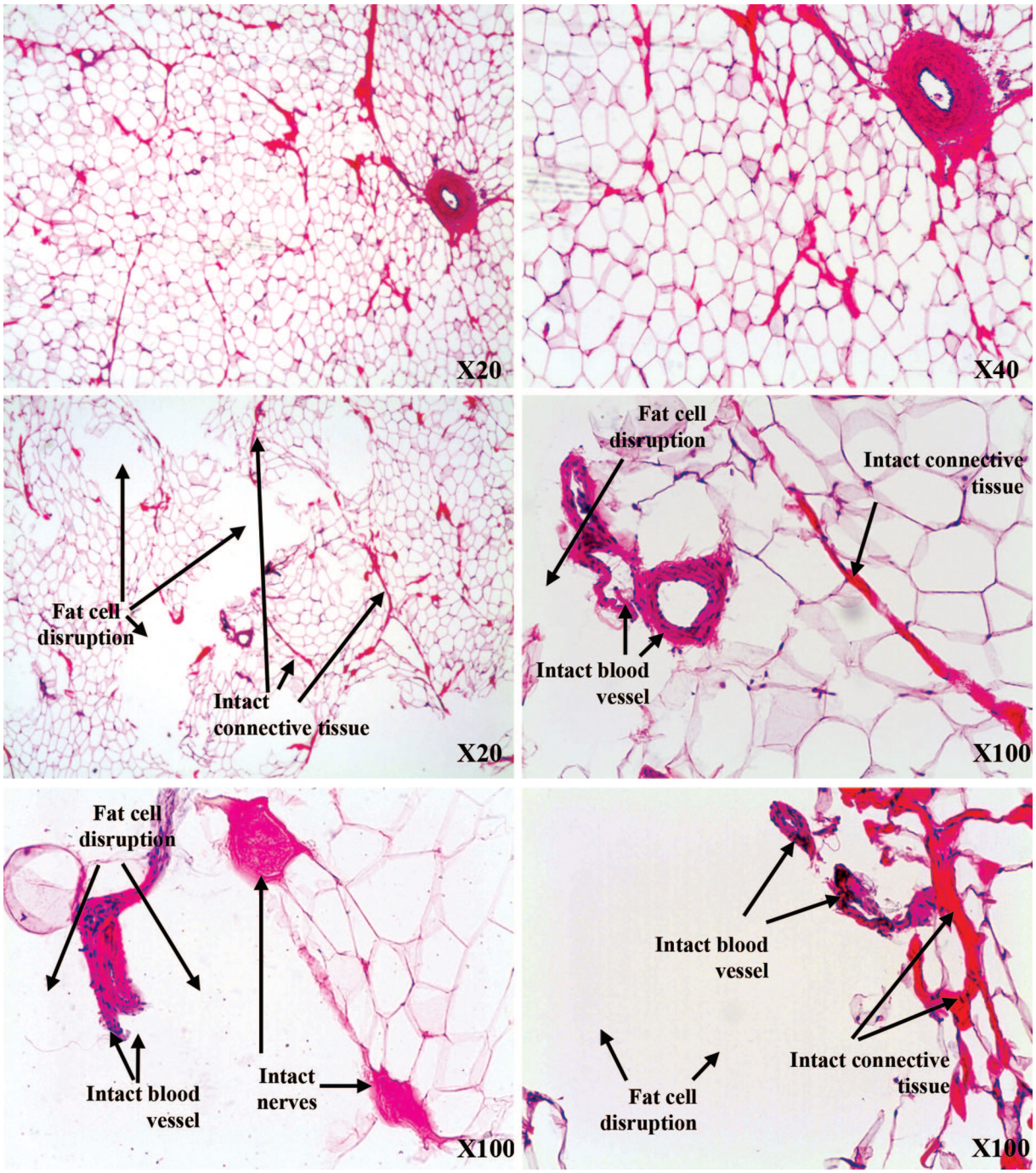

Fig. 8. Microscopic evaluation of the adipose tissue. While intact fat cells are observed in the untreated control (*above*), fat damage is detected in the ultrasound-treated samples (*center* and *below*), where ultrasound leads to selective adipocytes disruption, leaving connective tissue (*center*), blood vessels (*center, right*, and *below*) or nerve (*below, left*) intact.

duced cell destruction. In summary, the ultrasonic energy signature was consistent with initial cavitation followed by the mechanical destruction of cells.

The porcine model is an appropriate model for examining the effects of ultrasonic energy on skin and other organ systems.[18] Initial safety studies examined whether the ultrasonic energy would harm the epidermis. From the laboratory experiments summarized above, very low levels of acoustic energy were expected. This was confirmed in the porcine model, in which ultrasonic energy did not produce adverse events if an appropriate amount of fat thickness was present, as confirmed by either cell viability or tissue stains. Blinded observers could not distin-

guish a treated versus an untreated specimen when viewing only the histologically stained epidermal portion of prepared skin sections.

The data were consistent with mechanical disruption of adipocytes by mechanical forces. Histological assessments of multiple experiments using many animals consistently show discrete holes either at a gross tissue level or from a more magnified view of adipocytes. Using standardized formalin-fixed specimens, the incubation time allows the small cluster of tissue destruction zones to be closed or compressed, while the rapid-freeze processing allowed the ultrasonically treated skin specimens to maintain the altered structure. Adipocytes occupy the majority of space in this anatomical compartment, and the majority of destruction would be to adipocytes. If endothelial cells in this anatomical area were lysed by cavitation, single endothelial cells might be destroyed, but the actual damage to a blood vessel would be minimal, thus preventing loss of vascularity in the treated zone. The current tested stains could not distinguish viable from nonviable endothelial cells. However, in support of this concept, no gross bleeding was associated with treated tissue in the subcutaneous or dermal zones.

The results presented here represent more than 16 months of experiments performed at the UltraShape research facilities and involved multiple devices, numerous transducers, and multiple users. The senior author (S. A. B.) was present for critical bench experiments and reviewed all primary data obtained by the UltraShape-affiliated scientists. All of the results have been consistent over time, even in the presence of these several potential preanalytical confounders. This technology platform and the associated hardware were reliable.

An important finding in all the tested models was the relatively consistent size and shape of the ultrasonic treatment zones. Examinations of the respective focal lengths and dimensions of the initial fluidic determinations (20 mm × 8 mm), the phantom models (18 mm × 9 mm) and the porcine model (10 mm × 6 mm) shows that the treatment areas were similar, notwithstanding that compression of the treatment zone in a denser animal tissue environment and specimen contracture in fixed histological specimens are expected in comparison to what is seen in fluids or gels.

The consistent results observed among the various test technologies and porcine animal model provide a strong framework for understanding how the energy is being delivered in a focused, cavitation-associated manner and what immediate tissue results one may expect from a single application of the noninvasive focused ultrasonic energy. However, these observations do not lead directly to being able to predict clinical results, as the porcine skin differs in minor quantities from human skin characteristics with regard to dermal thickness and fat deposition. Results from controlled clinical studies will be required, and these studies are ongoing in the United States.

The introduction of a novel technology platform utilizing a new energy form requires a rigorous preclinical examination of both safety and efficacy. Utilizing advanced fluidic and tissue-mimicking modeling systems with ultra–high-speed cameras, the initial designs of a team of physicists, scientists, material specialists, and software and hardware researchers were tested and confirmed. In conclusion, we can state that (1) a noninvasive focused ultrasonic device was developed to deliver energy within a definable treatment zone at a depth that was clinically targeted (the adipose tissue layer of interest for body-contouring applications) and (2) the energy from this device is delivered as cavitation and not as thermal energy, which has very important clinical implications for wound healing. Finally, a safe and effective delivery of noninvasive focused ultrasonic energy that may be applied clinically for body contouring is fully supported by the laboratory and preclinical data presented in this report.

Spencer A. Brown, Ph.D.
Department of Plastic Surgery
University of Texas Southwestern Medical Center
5323 Harry Hines Boulevard
Dallas, Texas 75390
spencer.brown@utsouthwestern.edu

ACKNOWLEDGMENTS

All products were supplied by UltraShape Inc., and experimental procedures and preclinical studies were performed at the UltraShape Inc. facilities or in a preclinical testing laboratory.

REFERENCES

1. American Society of Plastic Surgeons. 2000/2006/2007 National Plastic Surgery Statistics: Cosmetic and Reconstructive Procedure Trends. Available at: http://plasticsurgery.org/media/statistics/loader.cfm?url=/commonspot/security/vgetfile.cfm&PageID=29287. Accessed September 15, 2008.
2. ASPRS Task Force on Lipoplasty, J. G. Bruner (Chair). 1997 Survey Summary Report. Arlington Heights, Ill.: American Society of Plastic and Reconstructive Surgeons, 1998.
3. Co AC, Abad-Casintahan MF, Espinoza-Thaebtharm A. Submental fat reduction by mesotherapy using phosphatidylcholine alone vs phosphatidylcholine and organic silicium: A pilot study. *J Cosmet Dermatol.* 2007;6:250–257.
4. Grazer FM, de Jong RH. Fatal outcomes from liposuction: Census survey of cosmetic surgeons. *Plast Reconstr Surg.* 2000; 105:436–446, discussion 447–448.

5. Sadick N, Magro C. A study evaluating the safety and efficacy of the VelaSmooth system in the treatment of cellulite. *J Cosmet Laser Ther.* 2007;9:15–20.
6. Moreno-Moraga J, Valero-Altés T, Riquelme AM, Isarria-Marcosy MI, de la Torre JR. Body contouring by non-invasive transdermal focused ultrasound. *Lasers Surg Med.* 2007;39: 315–323.
7. Teitelbaum SA, Burns JL, Kubota J, et al. Noninvasive body contouring by focused ultrasound: Safety and efficacy of the Contour I device in a multicenter, controlled, clinical study. *Plast Reconstr Surg.* 2007;120:779–789, discussion 790.
8. National Electrical Manufacturers Association. *Acoustic Output Measurement Standard for Diagnostic Ultrasound Equipment, NEMA UD 2-1992.* Rosslyn, Va.: NEMA, 1992.
9. Raman CV. The diffraction of light by high frequency NATH, NSN ultrasonic waves. *Proc Indiana Acad Sci.* 1935;2:406.
10. Hanafy A, Zanelli CI. Quantitative real-time pulsed Schlieren imaging of ultrasonic waves. *Proceedings of the IEEE Ultrasonics Symposium.* 1991;2:1223–1227.
11. Luna Lee G. *Histopathologic Methods and Color Atlas of Special Stains and Tissue Artifacts.* Downers Grove, Ill.: Johnson Printers; 1992:151–152.
12. Lynch MJ, Raphael SS, Mellor LD, Spare PD, Inwood MJ. *Medical Laboratory Technology and Clinical Pathology.* 2nd ed. Philadelphia: W.B. Saunders; 1969.
13. Van Noorden CJ, Vogels IM. Cytophotometric analysis of reaction rates of succinate and lactate dehydrogenase activity in rat liver, heart muscle and tracheal epithelium. *Histochem J.* 1989;21:575–583.
14. Guillory RK, Gunter OL. Ultrasound in the surgical intensive care unit. *Curr Opin Crit Care* 2008;14:415–422.
15. Lockhart ME, Robbin ML. Renal vascular imaging: Ultrasound and other modalities. *Ultrasound Q.* 2007;23:279–292.
16. Ferraro GA, De Francesco F, Nicoletti G, Rossano F, D'Andrea F. Histologic effects of external ultrasound-assisted lipectomy on adipose tissue. *Aesthetic Plast Surg.* 2008; 32:111–115.
17. Leslie TA, Kennedy JE. High-intensity focused ultrasound principles, current uses, and potential for the future. *Ultrasound Q.* 2006;22:263–272.
18. Paddock HN, Schultz GS, Mast BA. Methods in reepithelialization: A porcine model of partial-thickness wounds. *Methods Mol Med.* 2003;78:17–36.

English Language Assistance for Authors

Appropriate use of the English language is a requirement for publication in *Plastic and Reconstructive Surgery.* Authors who have difficulty in writing English may seek assistance with grammar and style to improve the clarity of their manuscript. Many companies provide substantive editing via the Web. Website addresses for these companies include:

- www.biosciencewriters.com
- www.bostonbioedit.com
- www.sciencedocs.com
- www.prof-editing.com
- www.journalexperts.com
- www.themedicaleditor.com

Please note that neither the American Society of Plastic Surgeons nor the *Journal* takes responsibility for, or endorses, these services. Their use does not guarantee acceptance of a manuscript for publication.